Correlation among Solidification Process, Microstructure, Microsegregation and Solidification Cracking Susceptibility in Stainless Steel Weld Metals†

Seiji KATAYAMA*, Takuhiro FUJIMOTO** and Akira MATSUNAWA***

Abstract

This study was undertaken on about 60 Fe-Cr-Ni ternary stainless steels to obtain a better understanding of the effect of primary and eutectic delta(δ)-ferrite on cracking resistance with the object of developing a highly crack-resistant alloy by defining a correlation between solidification process and cracking susceptibility. According to the microstructural observation of weld metals quenched rapidly from high temperatures during TIG welding and normal weld metals cooled continuously to room temperature after welding, solidification processes and related microstructures of stainless steel weld metals were classified into five different types and correspondingly eight characteristic modes, respectively. It was noted that a small content of residual δ-ferrite at room temperature resulted from primary ferrite in cell axes (Mode VF (vermicular ferrite) and Mode LF (lacy ferrite)) for lower Cr and Ni equivalents, while it came from eutectic ferrite at solidification grain and cellular dendritic boundaries (Mode IF (intercellular eutectic ferrite)) for higher Cr and Ni equivalents.

Solidification crack susceptibility was assessed by the BTR (solidification brittleness temperature range) in the Trans-Varestraint test and L_T (total crack length) in TIG and resistance spot welds. It was found that there was a close relationship between solidification cracking susceptibility and solidification process: Type A (austenitic single-phase solidification) – Mode FA (fully austenitic structure) steels were the most susceptible to cracking and Type FE (primary ferrite and eutectic ferrite-austenite solidification) – Mode VF (vermicular ferrite) or Mode LF (lacy ferrite) weld metals were the most resistant. It was therefore confirmed that an austenitic stainless steel containing only 2% residual δ-ferrite exhibited an excellent resistance to cracking due to Type FE solidification process. Moreover, it was revealed that some Type AE (primary austenite and eutectic austenite-ferrite solidification) – Mode IF materials were resistant and the reason was attributed to the beneficial effects of eutectic ferrite on the decrease in microsegregation of P and the resistance to cracking propagation.

KEY WORDS: (Austenitic Stainless Steels) (Weld Metals) (Ferrite) (Solidification) (Metallography) (Inclusions) (Hot Cracking) (Weldability Tests) (Microstructure)

1. Introduction

It is well known that fully austenitic stainless steel weld metals are very susceptible to hot cracking although they possess excellent corrosion resistance and good mechanical properties.[1),2)] The conventional guideline to prevent this hot cracking has recommended that weld metal should contain about 5% or more of residual δ-ferrite.[1)]

A large number of intensive studies[3)–43)] have been conducted for the purpose of determining the effective amount of δ-ferrite, elucidating the beneficial effect of δ-ferrite and the mechanism of hot cracking, and improving cracking susceptibility. Hull[3)] showed that stainless steel alloys containing 5 to 10% δ-ferrite in the as-cast microstructure were most resistant to hot cracking. Arate, et al.[4)] and Kawashima, et al.[5)] confirmed that cracking susceptibility was decreased with an increase in ferrite content from 0 to 6 or 10%. Lundin, et al.[6),7)] demonstrated that the ferrite levels required to prevent fissures (cracks) were different among the AISI/AWS types of austenitic stainless steels: for example, 2.5FN or more and 6FN or more for Type 316 and 347, respectively. Brooks[8)] further indicated that the amount of δ-ferrite required to eliminate cracking in AISI 309 weld metals was dependent on P and S contents.

It has been verified by the fractographic technique that solidification cracking and liquation cracking take an important role of hot cracking in weld metal and the HAZ or reheated-zone, respectively.[9)–13)] In some recent studies,[11),14)–40)] based on the concept that the cracking takes place at elevated temperatures during and just after

* Research Instructor
** Former Graduate Student, now with Sumitomo Heavy Industries, Ltd.
*** Associate Professor

Transactions of JWRI is published by Welding Research Institute of Osaka University, Ibaraki, Osaka 567, Japan

solidification, the effect of δ-ferrite on the reduction in cracking susceptibility has been interpreted in terms of the solidification process and its related δ-ferrite behavior rather than the residual ferrite content at room temperature. Masumoto, et al.[14] suggested that the effect of ferrite was ascribed to the primary solidification of ferrite. Matsuda, et al.[15)-22)] indicated that duplex ferritic-austenitic AISI 304 stainless steels are superior in cracking resistance to fully austenitic AISI 310S and fully ferritic AISI 430 stainless steels, and have proposed that the excellent cracking resistance of ferritic-austenitic stainless steels such as AISI 304 can be basically understood by considering that the irregular (migrated) grain boundaries, which are formed during solidification and subsequent cooling, have good ductility or resistance to the propagation of cracking in addition to the beneficial effect which the primary δ-ferrite solidification has on the decrease in the microsegregation of impurities such as P and S. They also defined the cracking mechanism and the detrimental effect and its degree of P and S on the cracking in AISI 310S weld metals.[10),11),19)-21)] Suutala, et al.[27)-31)] reported a correlation between the room temperature microstructure and the solidification mode of weld metal, and confirmed that duplex ferritic-austenitic solidification in welds produced the minimum cracking susceptibility. Lippold, et al.[33)-35)] indicated four specific compositional regions exhibiting a respective characteristic ferrite morphology and the effect of solidification behavior on hot cracking susceptibility. Backfilled or healed cracks were observed.[21),30)-32),35)] Brooks, et al.[38)] emphasized the role of the complex crack path encountered along δ-γ boundary in the high cracking resistance of primary ferrite solidified welds, which seems similar to the proposal made by Matsuda, et al.[11),18)-20)] As quoted above, a good understanding of solidification processes, solidification behavior of δ-ferrite and the effect of primary δ-ferrite on cracking resistance has been obtained. There are, however, few papers explaining satisfactorily the effects of eutectic ferrite on the microsegregation of impurities and on the cracking resistance.

The objective of this investigation is to confirm the correlation among the solidification process, microstructural mode, microsegregation degree of P and S at boundaries and cracking susceptibility in stainless steel weld metals. Further aims are to define the beneficial role of primary and/or eutectic ferrite in reducing cracking and to offer the fundamentals for development of crack-resistant alloys.

2. Materials and Experimental Procedure

2.1 Materials used

Materials used are 41 heats of Fe-Cr-Ni ternary stainless steels ($100^{l}x100^{w}x3^{t}$ mm or $100^{l}x50^{w}x5^{t}$ mm) containing 13–32%Cr and 5–24%Ni with commercial levels of other elements. These steels were selected to provide both different solidification processes and various ferrite contents[27)-31),42)] and produced by adding suitable amount of pure Cr, Ni or Fe to the base metals of AISI 304 or 310S so as to cover wider compositional ranges than compositions used by Suutala, et al.[27)-30)] More materials investigated are 8 commercial stainless steels to obtain the reference data of solidification process and δ-ferrite content, and 4 heats of Fe-Cr-Ni ternary alloys with very low levels of P, S and other elements to define the effect of solidification process on cracking susceptibility. Furthermore, 8 heats of stainless steels with about 0.33%P or 0.27%S adopting 4 different solidification processes were employed to confirm the effect of primary and/or eutectic δ-ferrite on the microsegregation of P and S during solidification in weld metals and on cracking susceptibility. The position of materials, some of which are listed in **Table 1**, is illustrated in the Schaeffler diagram in **Fig. 1**. In this figure the numerals near the marks show the residual δ-ferrite content in % measured by the Ferrite Scope in as-cast experimental specimens (with 30% or more of ferrite) or in TIG weld metals made under I= 100A, E=12.5V and v=150mm/min. The measured ferrite contents are fairly consistent with the ferrite contents predicted from the Schaeffler diagram.

Table 1 Chemical Compositions of some materials used.

(a) Experimental Fe-Cr-Ni ternary stainless steel alloys

Heat No.	Chemical composition (wt%) Cr	Ni	P	S	Cr_{eq} (%)	Ni_{eq} (%)
1	15.85	10.90	0.030	0.008	16.48	13.54
2	16.80	9.85	0.021	0.008	17.45	11.96
3	18.00	9.35	0.034	0.008	18.71	11.63
4	18.85	8.15	0.031	0.008	19.54	10.88
5	22.40	5.90	0.023	0.009	22.86	8.00
6	24.70	19.30	0.022	0.003	25.50	21.35
7	25.75	18.05	0.021	0.004	26.57	19.97
8	26.50	17.10	0.020	0.004	27.22	18.97
9	26.85	16.60	0.020	0.004	27.54	18.87
10	28.10	15.30	0.018	0.005	28.85	17.41
11	31.75	11.70	0.015	0.007	32.25	13.48
12	25.30	21.85	0.002	0.010	25.33	22.13
13	26.75	20.05	0.002	0.010	26.82	20.26
14	27.70	18.35	0.002	0.011	27.74	18.57
15	32.15	12.85	0.002	0.012	32.18	13.06

1 - 11: C=0.03-0.05 (%), Mn=0.95-1.60, Si=0.30-0.55, N=0.015-0.025

12 - 15: C=0.006-0.008 (%), Mn=0.003, Si=0.005

(b) Commercially available stainless steels

Materials (SUS, AISI)	Chemical composition (wt%) C	Si	Mn	P	S	Cr	Ni	Cr_{eq} (%)	Ni_{eq} (%)
Type 310S	0.07	0.61	1.69	0.017	0.002	25.02	19.16	25.94	22.11
Type 304	0.07	0.45	0.82	0.025	0.005	18.16	8.63	18.84	11.14
Type 309	0.06	0.76	1.62	0.031	0.002	22.16	14.16	23.30	16.77

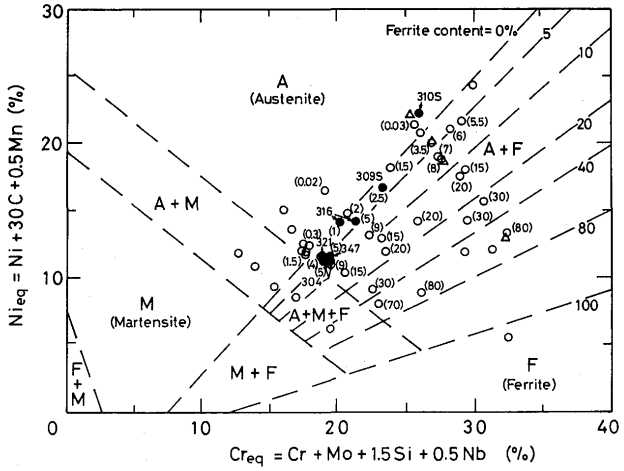

Fig. 1 Location of materials relative to Schaeffler diagram.

2.2 Hot cracking tests

The Trans-Varestraint test and the other practical cracking tests by using TIG arc spot welding or resistance spot welding were conducted to assess solidification cracking susceptibility.[11),15),17),24)]

The Trans-Varestraint test[43)] was carried out at augmented-strains(ϵ) of about 0.5 and 4% at strain rates of 20% or more, when TIG bead-on-plate welding was performed on 5 mm thick plates under the conditions of I= 150A, E=15V and v=100 mm/min and on 3 mm thick sheets under I=100A, E=12.5V and v=150 mm/min. The length of cracks or backfilled cracks was measured by both reading binocular microscope and the SEM. Cracking susceptibility was evaluated by the BTR (solidification brittleness temperature range), which was obtained by combining the maximum crack length with the cooling curve measured near the center of weld bead.

TIG arc spot welding cracking test was done on 100^{l}x 50^{w}x5^{t} mm plates under the conditions of I=300A, E=20V and t=2s. The length of cracks observed on a nugget surface was measured by reading binocular microscope, and the total crack length was used as an index of a practical cracking propensity. Resistance spot welding cracking test was performed by using piled-up two sheets of 30^{l}x30^{w}x3^{t} mm under the conditions of P=1300kg, I=10.9 to 11.6kA and t=22c/s. The total crack length (L_T) measured on the cross section of a weld nugget was used to compare a practical cracking tendency.

2.3 Metallographic and fractographic examination

Solidification processes and solidification modes of stainless steel weld metals were determined by the microstructural observation of weld metals which were water-quenched from high temperatures during quasi-stationary TIG welding[15)] and cooled continuously to room temperature after welding. Phosphide and sulphide contents (counts) in weld metals of typical different solidification processes, resulting from the microsegregation of P and S at boundaries, were measured by the point counting method[13)] or by the SEM (scanning electron microscope) with the EDX (energy dispersive X-ray spectroanalyser).[19)] The liquidus (T_L) and solidus (T_S) of materials were measured by thermal analyses.[16)] The fracture surfaces of cracks produced in the Trans-Varestraint test were observed and analyzed by the SEM.[23)]

3. Experimental Results and Discussion

3.1 Correlation among solidification process, solidification mode and microstructure of weld metals

Since solidification cracking occurs near the solidus during fusion welding, it would be essential to know the fundamentals of solidification process and its related microstructure of ferrite-austenite behavior in stainless steel weld metal close to temperatures over which cracking initiates and propagates. The Fe-Cr-Ni ternary phase diagrams are useful in understanding the solidification process and related microstructure. **Figure 2** (a) illustrates

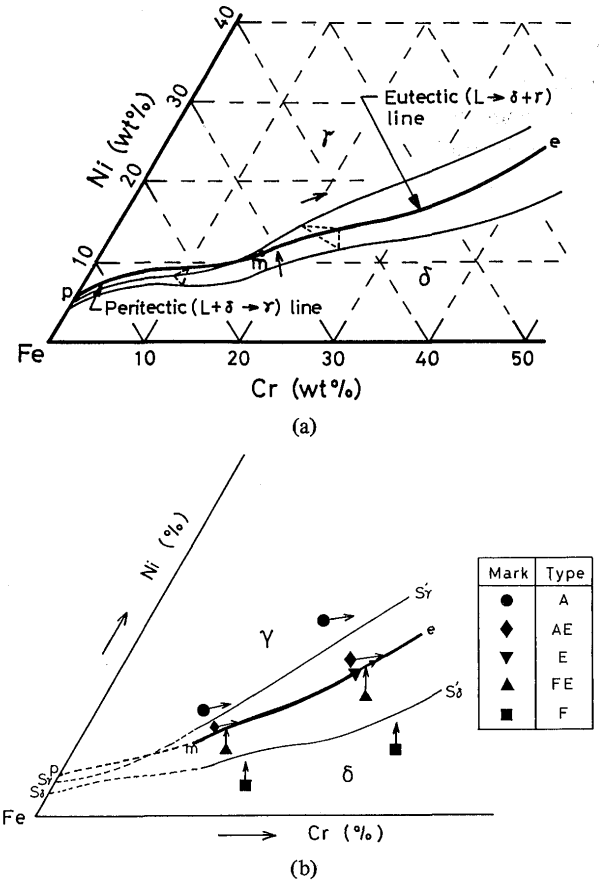

Fig. 2 Projection of liquidus and solidus surface near Fe-rich corner of Fe-Cr-Ni ternary system diagram (a) and its qualitative schematic diagram (b) showing predicted direction of liquid compositional changes during solidification of each type of material.

the projection of the liquidus and solidus surfaces near the Fe-rich corner of the ternary diagram,[44)-46)] whose qualitative schematic diagram is shown in Fig. 2 (b). The line pme in Fig. 2 is a border line on the liquidus surface. The primary solidification of austenite (γ) occurs all over the compositions of Ni-rich side of the line, and that of δ-ferrite (δ) does on the Cr-rich side. The peritectic reaction ($L+\delta \rightarrow \gamma$) takes place at the compositions along the line pm, while the eutectic reaction ($L \rightarrow \gamma + \delta$) occurs at the compositions along the line me. Because the composition of the transient point m is about 17%Cr-9.5%Ni-Fe[45)] (15%Cr-10%Ni-Fe),[38),44)] the solidification processes of most stainless steels are reasonably classified into 5 distinct types: Type A of the austenitic single-phase solidification, Type AE of the primary austenite and eutectic austenite-ferrite solidification, Type E of the eutectic solidification of ferrite and austenite, Type FE of the primary ferrite and eutectic ferrite-austenite solidification (including divorced eutectic ferrite or partly peritectic solidification) and Type F of the ferritic single-phase solidification. Representative compositions are indicated as different marks (●, ◆, ▼, ▲, ■) in Fig. 2 (b), the arrows of which present the direction of liquid compositional changes during solidification.[11),15),29),47),48)] It is noted that the direction of liquid compositional changes is different between primary austenite and primary ferrite. Liquid compositions of Type FE and Type F materials showing normally complex ferrite morphology vary to the direction of the increase in Ni content along nearly-constant Fe contents. **Figure 3** (a) and (b) show schematic

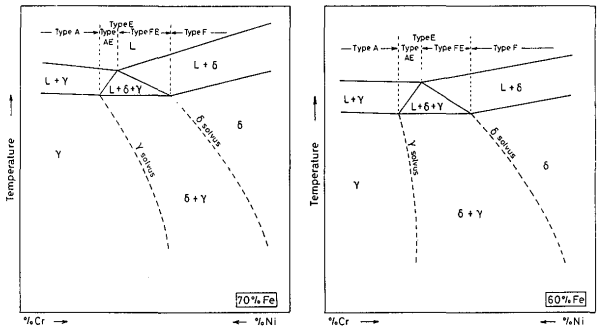

Fig. 3 Schematic Fe-Cr-Ni pseudo-binary diagrams at 70%Fe (a) and at 60%Fe (b).

pseudo-binary vertical sections of Fe-Cr-Ni ternary phase diagram at 70 and 60%Fe on the basis of other literature.[14),21),33),49)-51)] The solidification process and related microstructure of weld metal can be affected and altered by segregation of alloying elements during non-equilibrium solidification at higher cooling rates,[34),52)-55)] but it is understood from these cross-sectional diagrams that the solidification and subsequent transformation of stainless steel take place according to one of the above-mentioned five different solidification types, and resultantly that various morphologies of δ-ferrite observed in the microstructure are brought about during cooling through the ($\delta + \gamma$) phase field. It is apparent that γ solvus for higher Fe (lower Cr+Ni) content such as 70%Fe varies more largely from high Ni (low Cr) content to low Ni (high Cr) content with a drop in temperature than for lower Fe (higher Cr+Ni) content. This means that a large portion of primary and eutectic δ-ferrite is easier to transform to austenite and to disappear at higher Fe (lower Cr+Ni) content.[21)]

A number of recent studies,[15),20),27)-41)] which have been devoted to the understanding of the solidification process and the origin of complex ferrite morphologies, are conducive to the interpretation of complicated microstructures, although the names of characteristic microstructures are different and confused among some researchers[3),27),34),38),40)] (the comparison will be summarized in Table 2) and the interpretation of the transformation mechanism of ferrite to austenite is still in a controversy.[34),41),56)]

In this study, therefore, as-cast and as-welded microstructures of stainless steels were carefully observed on the basis of the microstructures classified in previous studies[27)-40)] and their correlation to solidification processes was investigated. **Figure 4** (a) to (f) show typical

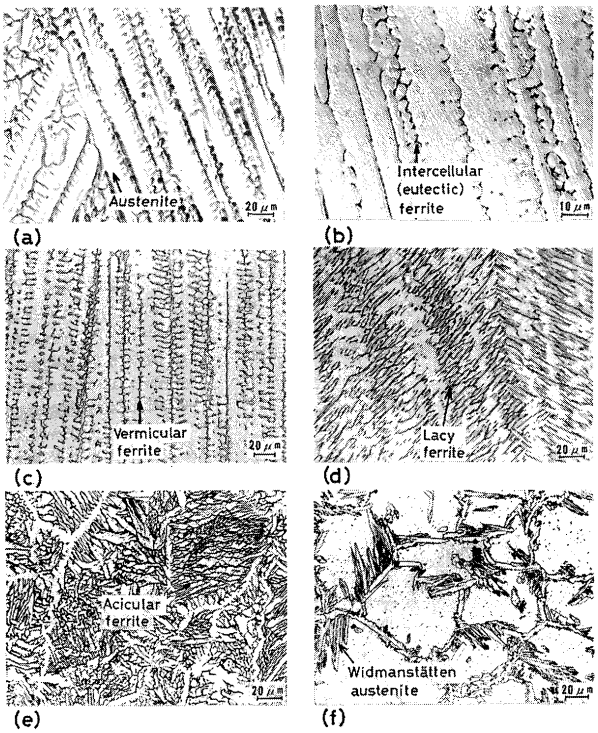

Fig. 4 Typical weld metal microstructures of stainless steels:
(a) fully austenitic cellular dendritic microstructure (Mode FA);
(b) intercellular eutectic ferrite (Mode IF);
(c) vermicular (dendritic or skeletal) ferrite (Mode VF);
(d) lacy ferrite (Mode LF);
(e) acicular (lathy) ferrite (Mode AF);
(f) Widmanstätten (feathery) austenite (Mode WA).

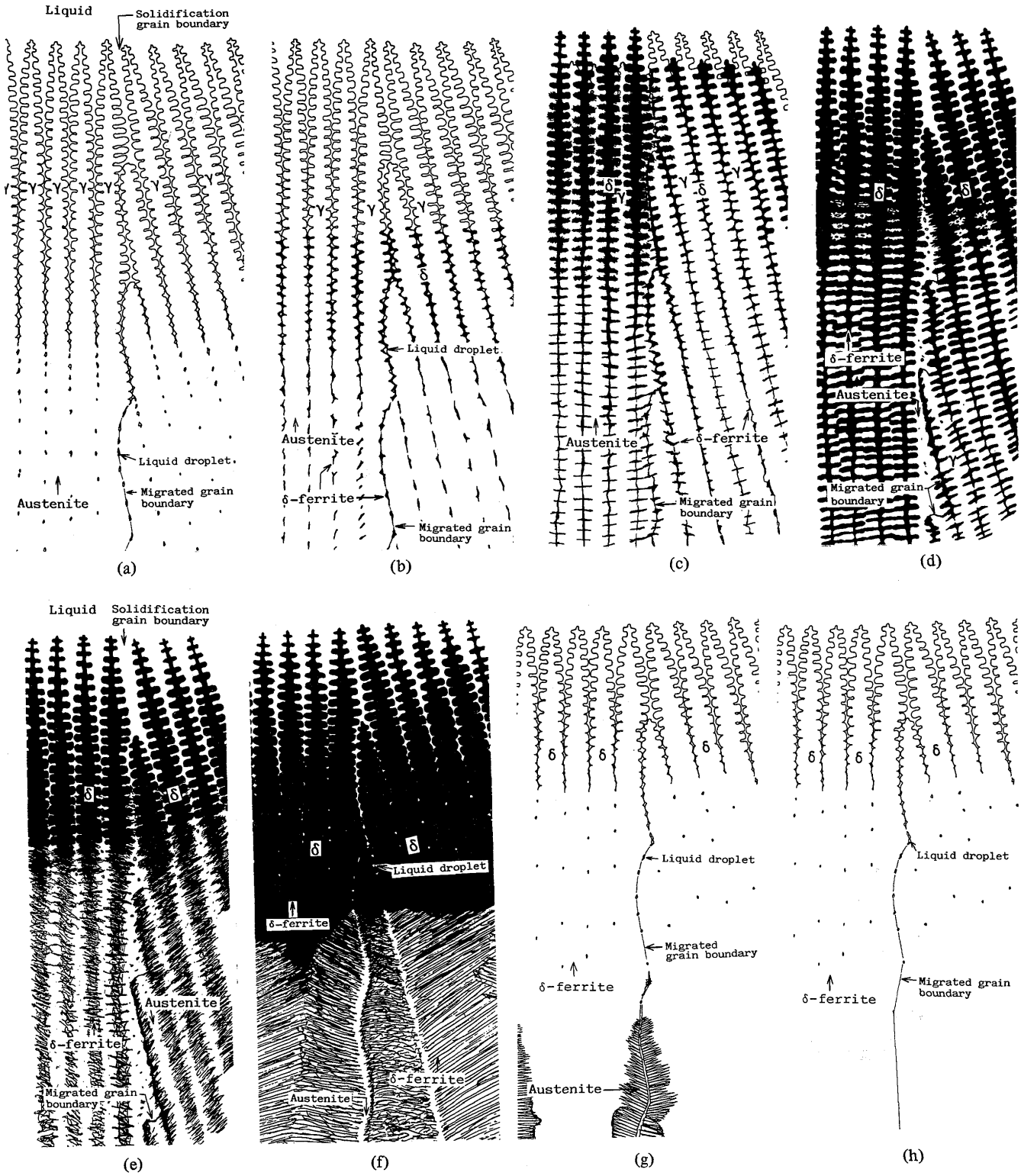

Fig. 5 Schematic representation of solidification and solid-state transformation behavior resulting in different characteristic morphologies of weld metal microstructures:
(a) Mode FA (fully austenite);
(b) Mode IF (intercellular eutectic ferrite);
(c) Mode EF (eutectic ferrite);
(d) Mode VF (vermicular ferrite);
(e) Mode LF (lacy ferrite);
(f) Mode AF (acicular ferrite);
(g) Mode WA (Widmanstätten austenite);
(h) Mode FF (fully ferrite).

microstructures of weld metals at room temperature. As seen in Fig. 4, it was found that the characteristic microstructures could be classified chiefly according to the appellation utilized by Lippold, et al.[34] and David.[40] Fig. 4 (a) shows fully austenitic cellular dendritic structure containing no ferrite, and the microstructural morphology is named Mode FA after fully austenite. In Fig. 4 (b) δ-ferrite is seen only at solidification grain and cellular dendritic boundaries, and Mode IF is named after intercellular (eutectic) ferrite. In Fig. 4 (c), (d) and (e), δ-ferrite is observed in the dendritic (vermicular or skeletal), lacy and needle-like (acicular) form, respectively. Mode VF, Mode LF and Mode AF are termed after vermicular ferrite, lacy ferrite and acicular ferrite, respectively. Fig. 4 (f) shows grain boundary austenite and feathery austenite growing from grain boundaries. The structure is called Mode WA after Widmanstätten austenite.

In order to further clarify the origins of these characteristic microstructures and their correlation to solidification processes, the observation of microstructures at solidification was conducted on weld metal rapidly quenched during TIG bead-on-plate welding.[15] Based on the observation result and partially on other studies,[11),20),30),38),40] the different characteristic morphologies of weld microstructures during solidification and subsequent cooling are shown schematically for a wide range of stainless steel compositions in **Fig. 5**. The variation in microstructure from Fig. 5 (a) to Fig. 5 (h) is generally observed in the order with an increase in Cr_{eq}/Ni_{eq}. The migrated grain boundaries are illustrated which will play an important role in path of solidification cracking propagation. The comparison of each typical microstructure to the respective solidification process is given in **Table 2**, together

Table 2 Correlation between distinct solidification processes and characteristic microstructural modes in stainless steels, and comparison with appellation used in other studies.

Creq/Nieq	Increase →							
Solidification process (Type)	L→L+γ→γ (A)	L→L+γ→L+γ+δ→γ+δ (AE)	L+γ+δ→γ+δ (E)	L→L+δ→L+δ+γ→δ+γ (FE)		L→L+δ→δ+γ (with δ→γ transf.) (F)		L→L+δ→δ
Characteristic microstructure (Mode)	Fully austenite (FA)	Intercellular (eutectic) ferrite (IF)	Eutectic ferrite (EF)	Vermicular ferrite (VF)	Lacy ferrite (LF)	Acicular ferrite (AF)	Widmanstätten austenite (WA)	Fully ferrite (FF)
		Globular ferrite (GF) Island-like ferrite (IF)						
N. Suutala T. Takalo T. Moisio				(Vermicular ferrite)	(Lathy ferrite)		(Lathy austenite)	
J. Lippold W. Savage		(Intercellular ferrite)		(Vermicular ferrite)		(Acicular ferrite)	(Widmanstätten austenite)	
S. David				(Vermicular ferrite)	(Lacy ferrite)	(Acicular ferrite)		
J. Brooks A. Thompson J. Williams	(Austenite)	(Eutectic ferrite)		(Skeletal ferrite)		(Lathy ferrite)	(Widmanstätten austenite)	

with the names used in other studies.[27)-30),34),36)-40] As shown in Fig. 5 and Table 2, Mode EF (eutectic ferrite) for the process of eutectic reaction L → L+δ+γ → δ+γ is illustrated and applied for difficult judgement on primary solidification of ferrite or austenite although it may be included in either Mode IF or Mode VF. Mode VF and Mode LF are considered for the Type FE solidification process, and Mode AF, Mode WA and Mode FF (fully ferrite) are termed for the Type F solidification process. Even in the same weld metal, however, mixed structure of Mode VF and Mode LF or Mode LF and Mode AF was frequently seen side by side, and the ratio of Mode VF to Mode LF or Mode LF to Mode AF appeared to increase with approach to the weld bead center line. There was also a possibility of the formation of vermicular ferrite (Mode VF) at room temperature formed from Type F solidification process when cooling rates are very slow.[15),33]

From the metallographic observation results of weld metals, the regions of each solidification process and related characteristic microstructures are indicated in the Schaeffler diagram in **Fig. 6** (a) and (b). In Fig. 6 (a) the open marks represent the results of the present study and the smaller solid marks are quoted from the results obtained by Suutala, et al.[27)-29)] In this study, the microstructures observed near the weld center are adopted as representative structure because cracking susceptibility

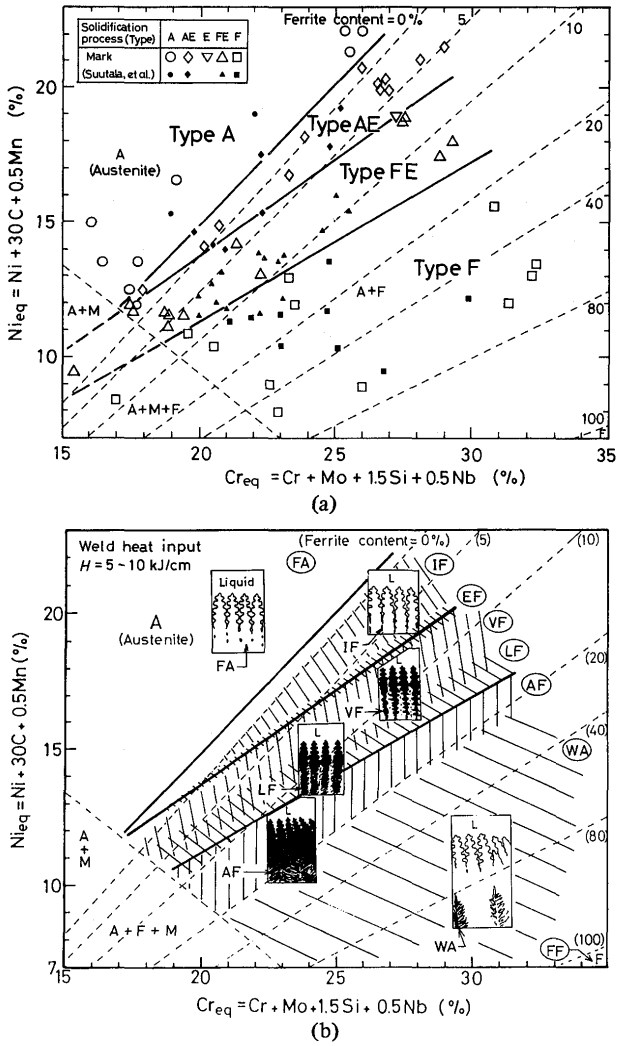

Fig. 6 Regions of solidification processes (a) and related characteristic microstructures (b) of stainless steel weld metals projected on Schaeffler diagram.

is evaluated by the BTR obtained from the length of maximum crack occurring near the bead center. It is noted that less than 5% predicted content of residual δ-ferrite is formed from Type FE solidification for materials with lower $Cr_{eq}+Ni_{eq}$ where the ferrite is retained as vermicular or lacy ferrite in the cellular dendritic cores of primary ferrite (as Mode VF or Mode LF), while a small amount of residual δ-ferrite for higher $Cr_{eq}+Ni_{eq}$ is formed from eutectic δ-ferrite at solidification grain and cellular dendritic boundaries (as Mode IF or Mode EF). In the case of about 10% residual δ-ferrite, Mode AF, mixed structure of Mode AF and Mode LF, mixed structure of Mode LF and Mode VF, and Mode VF are observed in this order with an increase in $Cr_{eq}+Ni_{eq}$. Besides, the residual δ-ferrite is thicker as $Cr_{eq}+Ni_{eq}$ content is larger. The residual δ-ferrite of more than 20% is normally formed as Mode WA from Type F ferritic single-phase solidification accompanied by the transformation of ferrite to austenite during cooling after solidification completion.

3.2 Correlation among solidification process, δ-ferrite content and solidification cracking susceptibility

The solidification cracking susceptibility of each weld metal was evaluated by the Trans-Varestraint test.[16] Typical cracks occurring in Type A (Mode FA) and Type AE (Mode IF) weld metals subjected to the Trans-Varestraint test are shown in **Fig. 7**. It is obvious that

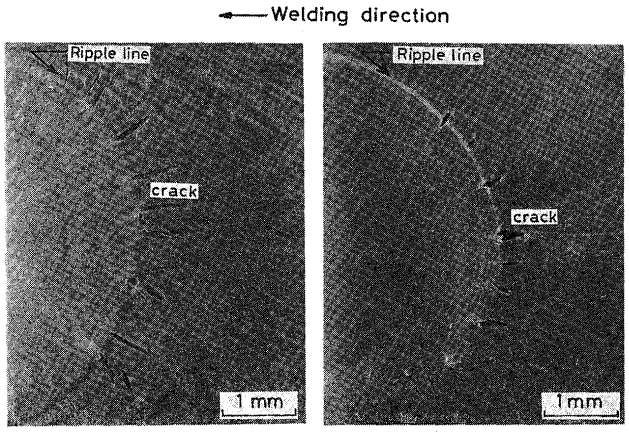

Fig. 7 Typical cracks in Type A (Mode FA) and Type AE (Mode IF) weld metals subjected to Trans-Varestraint test at ϵ=4%.
(a) Type A (Mode FA) weld metal
(b) Type AE (Mode IF) weld metal

Type AE (Mode IF) weld metal has smaller crack length than Type A (Mode FA) weld metal under the same strain of about 4%. This means that Type AE weld metal is more resistant to cracking than Type A weld metal. Since the BTR (solidification brittleness temperature range) is regarded as a more reasonable index of cracking susceptibility than the crack length, the BTR is obtained from the maximum crack length. The results of the BTR at $\epsilon \fallingdotseq 0.5$ and 4% are summarized in the Schaeffler diagram in **Fig. 8**

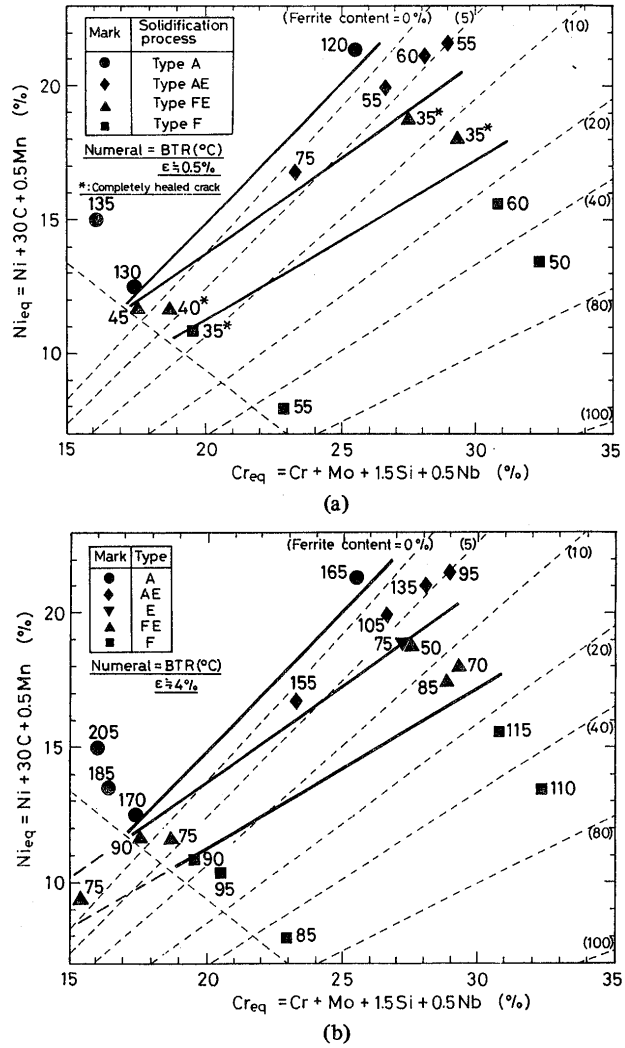

Fig. 8 Test results of BTR (°C) at ϵ=0.5% (a) and ϵ=4% (b) on Schaeffler diagram.

(a) and (b), where numeral at each solid mark shows the measured BTR. It is readily recognized that the BTR value increases in the order of Type FE, Type F, Type AE and Type A solidification. However, some of the Type AE materials show the similar BTR values to Type F stainless steels. Namely, some Type AE materials are fairly resistant to cracking. It is thus obvious that the cracking susceptibility is more closely related to the solidification process or microstructural morphology during weld-solidification than residual δ-ferrite content at room temperature predicted from the Schaeffler diagram. This result agrees well with that of Kujanpää, et al,[30),31)] except that some Type AE materials have been found to be fairly resistant to cracking. Here, particular emphasis should be put on the result that the material having lower Cr_{eq} side of lower $Cr_{eq}+Ni_{eq}$ in the compositional domain adopting Type FE solidification could be an excellent crack-resistant austenitic stainless steel with a very small content

or negligible content of residual δ-ferrite.

Figure 9 shows the relation between the BTR and

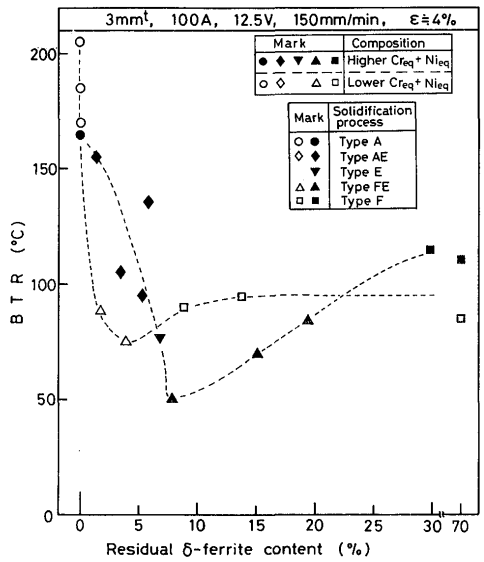

Fig. 9 Relationship between residual δ-ferrite content and BTR at ϵ=4% for lower and higher $Cr_{eq}+Ni_{eq}$ in stainless steel weld metals.

residual δ-ferrite content measured by the Ferrite Scope (or X-ray diffraction for high ferrite content) in weld metals. The narrow BTR is obtained in the residual δ-ferrite range from 7 to 20%. There exists a more distinct correlation between the BTR and residual δ-ferrite content in treating separately the data of lower and higher $Cr_{eq}+Ni_{eq}$ materials. A slight difference in the BTR among Type A solidification materials may be due to the influence of the difference in P and S contents, as discussed before.[19] The minimum BTR is observed at about 5% and 10% of ferrite content for lower and higher $Cr_{eq}+Ni_{eq}$, respectively, which shows that the best crack resistance can be achieved for Type FE solidification (Mode VF and/or Mode LF) with some amount of primary δ-ferrite. The BTR of less than 100°C can be obtained at only 2% or more of residual δ-ferrite for lower $Cr_{eq}+Ni_{eq}$ and between about 6 and 25% residual ferrite content for higher $Cr_{eq}+Ni_{eq}$. It is thus confirmed for lower $Cr_{eq}+Ni_{eq}$ that the great improvement of cracking susceptibility of fully austenitic stainless steel can be achieved at a smaller amount of residual δ-ferrite than 5% ferrite content recommended normally. This smaller amount of residual δ-ferrite for lower $Cr_{eq}+Ni_{eq}$ is attributed to the $\delta \rightarrow \gamma$ transformation that has almost completely occurred after Type FE solidification, as predicted from the variation in the γ solvus line which greatly extends toward the lower Ni (higher Cr) content with a drop in temperature in the pseudo-binary diagram in Fig. 3.

When augmented-strains applied in the Trans-Varestraint test are small, backfilled cracks are significantly observed in weld metals. The SEM microstructures and their schematics showing typical backfilled cracks are illustrated in **Fig. 10**. Completely and incompletely backfilled

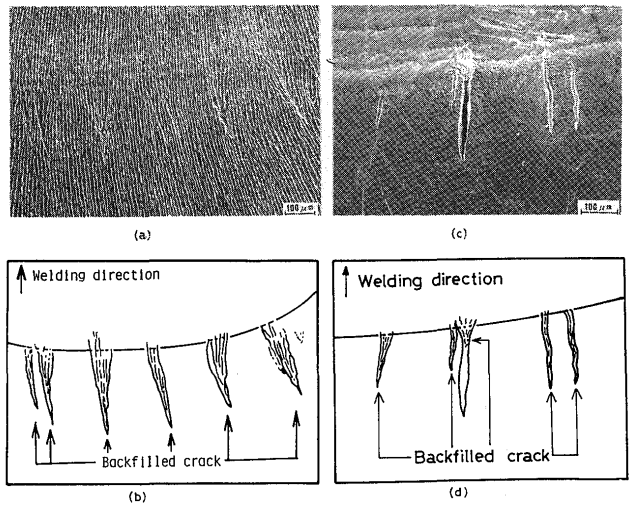

Fig. 10 SEM photos and their schematics of Type FE and Type F weld metals after Trans-Varestraint test, showing typical backfilled cracks.

(healed) cracks are seen at the location of the higher temperature side of solidification cracks in weld metals. These backfilled cracks observed in the Trans-Varestraint test imply that healing is probable to take place frequently in actual welds subjected to small strains and slow strain rates. Complete healing of cracks may result in an increase in the apparent ductility required to cause cracking. Therefore, the relationship between backfilled crack length and solidification crack length in each solidification process was investigated on two or three large cracks occurring near the weld bead center. The result is summarized in **Fig. 11**. All completely backfilled (healed)

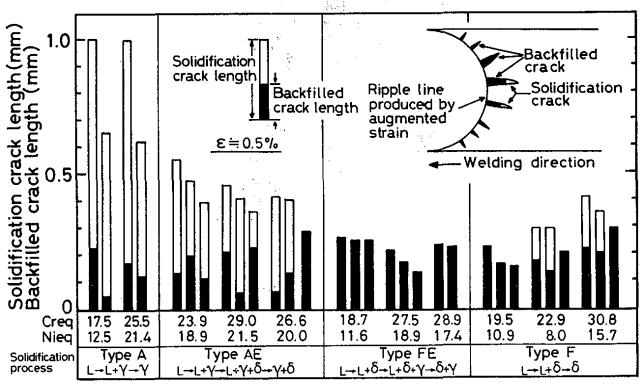

Fig. 11 Relation of backfilled cracks to solidification cracks in each solidification process of stainless steel, showing healing tendency of cracks.

cracks are observed in the cracks of less than 0.3 mm in length in the weld metals of Type FE and partly Type F solidification processes, but it can be judged that backfilled cracking is easier to occur in the case of shorter solidification crack length, although the effect of the

crack width on the formation tendency of backfilled cracks can not be recognized. Therefore, it would be essentially requested for development of excellent crack-resistant materials to produce materials which have shorter solidification crack length, in other words, narrower BTR.

Subsequently the relationship of the BTR to the nominal liquidus and solidus temperature was examined by using diagrams. **Figure 12** (a) and (b) show Fe-Cr-Ni pseudo-binary diagrams at $Cr_{eq}+Ni_{eq}=30\%$ and $Cr_{eq}+Ni_{eq}=46\%$, in which the lower temperature limits of the BTR at $\epsilon=0.5$ and 4% are illustrated (and the higher temperature limits of the BTR are the liquidus). These are non-equilibrium diagrams indicating the solidification processes classified by microstructural characteristics of weld metals although the liquidus and solidus are determined at a slow cooling rate of about 0.2°C/s in a crucible. The lower temperature limits of the BTR at $\epsilon=0.5$ and 4% vary similarly depending upon the increase in Cr_{eq} although the limits at $\epsilon=0.5\%$ are higher than those at $\epsilon=4\%$, and therefore these variation tendencies are apparently associated with the solidification process. For Type A solidification the temperature differences between the lowest temperature of the BTR and the solidus are the widest and the lower temperature limits extended largely below the solidus, but through Type AE process the lower temperature limits of the BTR are raised, which implies that the resistance of Type AE (Mode IF) material to cracking would be improved with an increase in eutectic δ-ferrite content. The BTR is minimum at a good combination of the primary δ-ferrite and eutectic δ-ferrite amounts in Type FE solidification. The lower temperature limits of the BTR for Type F process are lowered to some extent as compared with that for Type FE, but the difference between the solidus and the lower temperature limits of the BTR is nearly constant. It is especially interesting to notice that completely backfilled cracks or healing phenomenon can occur in TIG weld metals when the lower temperature limit of the BTR at $\epsilon=0.5\%$ is over 10°C higher than the solidus. This healing phenomenon may be explained by the "Shrinkage-Brittleness Theory"[57] or by "Generalized Theory"[58] insisting that cracks occurring above the coherent temperature or critical temperature can be healed. Therefore, it would be significant in producing crack-free practical weld metals to attain narrow BTR in the Trans-Varestraint test. In the study, to elucidate the mechanism of cracking propagation and its arrest would be essential to understand cracking susceptibility and the effect of δ-ferrite in preventing cracks. For these reasons, the solidification cracking mechanism in the Trans-Varestraint test was investigated by using AISI 310S, 304, etc.[10),18)] According to these studies,[10),16)–23)] the reason why the BTR of Type A weld metals is very wide is interpreted in terms of the mechanism that cracks occur at solidification grain boundaries above the solidus and propagate easily along migrated grain boundaries joining low solidification temperature liquid lakes below the solidus. As a result it is supposed that complete healing of cracks is impossible because of cracking propagation to a great extent below the solidus in Type A weld metals. The effect of eutectic δ-ferrite will be discussed on the basis of this concept in the

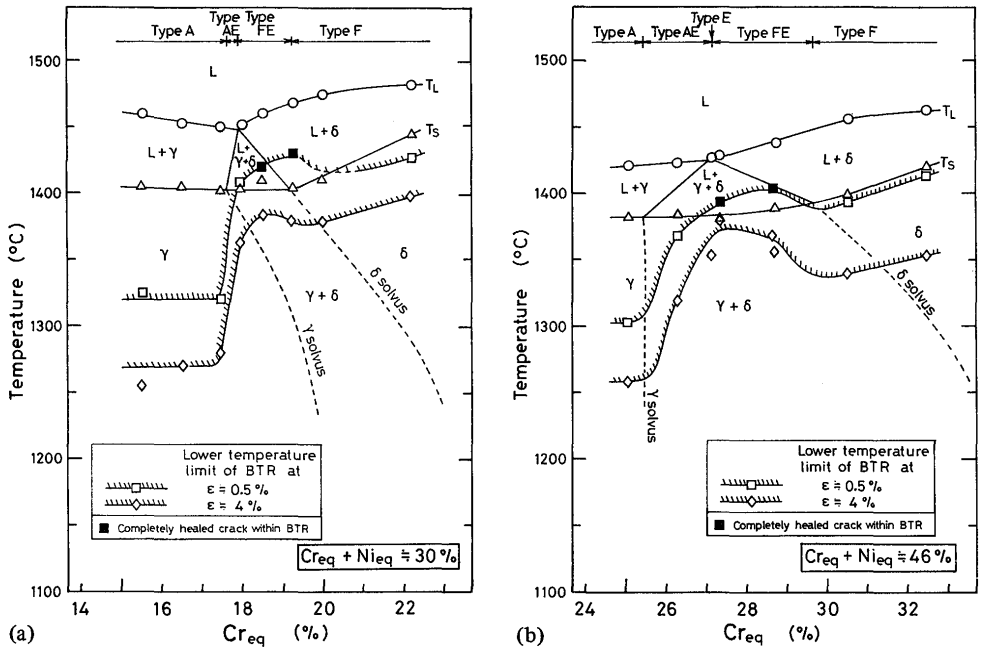

Fig. 12 Relation of lower temperature limits of BTR at $\epsilon=0.5$ and 4% to liquidus and solidus temperatures shown in pseudo-binary sections of stainless steel diagram at 30% (a) and 46% (b) $Cr_{eq}+Ni_{eq}$, showing effect of solidification process on backfilled, healed crack tendency and cracking susceptibility.

next sections 3.3 and 3.4.

TIG arc spot welding and resistance spot welding cracking tests were conducted on the specimens of each solidification process to evaluate cracking susceptibility in practical cases. Results are shown in **Fig. 13** and **14**. In TIG

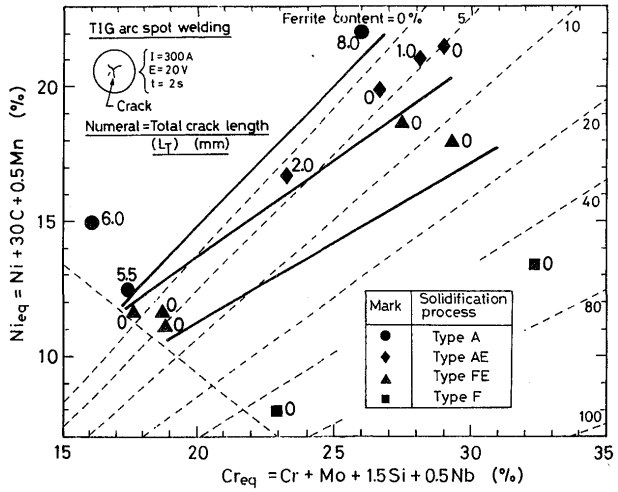

Fig. 13 Test results of total crack length in TIG arc spot welds on Schaeffler diagram, showing effect of solidification process on cracking susceptibility.

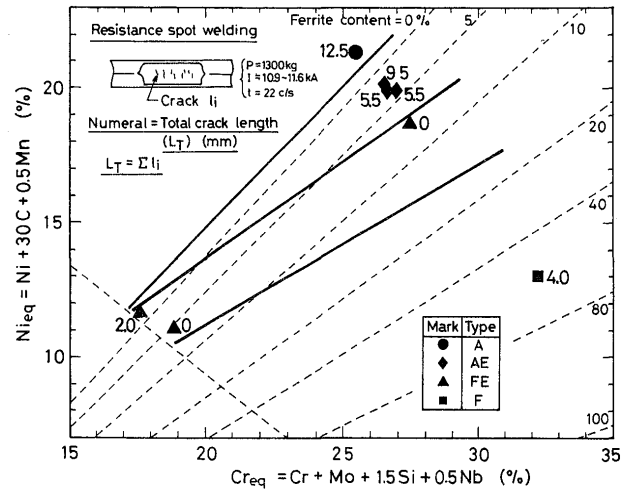

Fig. 14 Test results of total crack length in resistance spot weld cross sections on Schaeffler diagram, showing relation between solidification process and practical cracking propensities.

arc spot welding cracking test, as shown in Fig. 13, long cracks are observed in Type A materials and short cracks are found in some Type AE weld metals. However, no cracks occur in Type FE and Type F materials and the other Type AE steels, which have the BTR of less than 110°C at ϵ=4% in the Trans-Varestraint test. In resistance spot welding cracking test, the crack length decreases in the order of Type A, Type AE, Type F and Type FE solidification processes, and no cracks are observed in some Type FE weld metals which have the BTR of less than 40°C at ϵ=0.5% and less than 80°C at ϵ=4%. From the above results it was further confirmed that cracking tendencies in practice were closely associated with the solidification process in concord with the BTR evaluation: especially Type FE (Mode VF and/or Mode LF) materials with some amounts of primary δ-ferrite were most resistant to cracking, and Type AE (Mode IF) materials were more resistant to cracking than Type A (Mode FA) steels.

3.3 Microsegregation of P and S and their influence on cracking susceptibility for each solidification process

It would be important to know the degree of the microsegregation of P and S in understanding the relation of solidification process to solidification crack susceptibility. The microsegregation of P and S in Type 310S and Type 304 weld metals was investigated in details,[11),15)-21)] and the results confirmed that the primary δ-ferrite solidification had a noticeable effect on the reduction in the microsegregation of P and S. In this study, the investigation of P and S microsegregation to grain boundaries was further extended to each solidification process, and a particular interest was concentrated on the interpretation of the effect of Mode IF eutectic ferrite in Type AE.

In TIG weld metals with about 0.33%P or 0.27%S, P and S were found to segregate along solidification boundaries, where some phosphides enriched with P, Fe, Cr, Ni, etc. and some sulphides enriched with S, Mn and Cr were detected except for in Type F weld metal. In the case of about 0.33%P, phosphides were observed in a film-like shape at solidification grain boundaries and in rod-like and globular forms at cellular dendritic boundaries for Type A (austenitic single-phase solidification); phosphides were formed in film-like or granular shape in a row together with δ-ferrite at solidification grain boundaries for Type AE (primary austenite and eutectic solidification); a small number of phosphides were discovered in a rod-like form in the austenite phase corresponding probably to the last solidified parts for Type FE (primary ferrite and eutectic solidification); but no phosphides were detected for Type F (ferritic single-phase solidification). In the case of 0.27%S, sulphides were formed in a granular or globular form at austenitic solidification grain and cellular dendritic boundaries for Type A; sulphides for Type AE were observed together with δ-ferrite in a row at austenite solidification grain and cellular dendritic boundaries; sulphides for Type FE were seen in the austenite corresponding to the location of solidification grain and cellular dendritic boundaries; and sulphides for Type F were found in the ferritic grain and cellular dendritic boundaries. According to the above results, film-like phosphides were observed at grain boundaries only in Type A and Type AE weld metals. The reason is considered to be due to the high energy of a grain boundary and the formation of a large amount of low-melting-point liquid.[59)]

Subsequently, the segregated amounts of phosphides and sulphides in TIG weld metals with about 0.33%P and 0.27%S were measured by the point counting method. The results are tabulated for each solidification process in **Table 3**. Primary δ-ferrite in Type FE and Type F and eutectic δ-ferrite in Type AE exert a beneficial effect on a reduction in the microsegregation of P and S at solidification boundaries. The effect of primary δ-ferrite solidification on the decrease in P segregation is particularly remarkable.

Table 3 Effect of solidification process on formation tendency of phosphide and sulphide in weld metals with intentional addition of P and S.

Type of solidification process	A	AE	FE	F
Phase at solidification	γ	γ+(γ+δ)	δ+(δ+γ)	δ
P conent (%)	0.33	0.31	0.33	0.31
Area percent of phosphide(%)	2.91	1.36	0	0
S conent (%)	0.27	0.27	0.28	0.27
Area percent of sulphide (%)	1.68	1.50	1.45	1.09

In the papers dealing with the cracking susceptibility of stainless steel, a wide variety of materials have been used; such as, Fe-Cr-Ni ternary alloys with very small amounts of the other alloying elements, stainless steels with commercial levels of alloying elements, and materials doped with intentional contents of P and/or S. However, these materials were generally used separately in the respective studies. It would be therefore significant for the evaluation and better understanding of the solidification process and the effect of P and S on cracking susceptibility to compare the BTR (or cracking tendencies) among Fe-Cr-Ni ternary alloys and among materials with increased P or S contents solidifying in each solidification process.

Figure 15 shows a summary of the effects of P and S on the BTR at ϵ=0.5 and 4% for each solidification process. The addition of about 0.33%P widens the BTR for any solidification process. Especially the widening degree of the BTR with P addition is noticeable for the BTR at ϵ=0.5% of Type A and Type AE materials. This abrupt enlargement of the BTR can be interpreted in terms of the formation of considerable amounts of low-melting point liquids which solidify as film-like phosphides. The increase in S content from about 0.004 to 0.27% widens the BTR to some extent for any solidification process. It is obvious that 0.33%P widens the BTR to greater degree than 0.27%S for any solidification process, probably because the solidification temperature of P-rich liquid is much lower than that of S-rich liquid.[11),20)] Moreover, the results of Fe-Cr-Ni ternary alloys with very low contents of the other elements demonstrate that the BTR of alloys is apparently narrower than that of commercial steels for Type A and Type AE solidification. In other words, there is a possibility of the decrease in the BTR by reducing P contents only for Type A and Type AE solidification. From the above results it is summarized that the cracking susceptibility is enhanced in the orders of Type FE < Type AE < Type F < Type A for very low P content, Type FE < (Type AE, Type F) < Type A for commercial levels of P and S, Type FE < (Type F, Type AE) < Type A for high S content, and (Type FE, Type F) < (Type AE, Type A) for high P content. The reason why Type F materials are more resistant to cracking than Type A steels is readily attributed to the advantageous effect of primary δ-ferrite solidification on the reduction in the microsegregation of P in particular and S. It is also noted that the cracking resistance of Type AE materials containing commercial or lower contents of P is equal to or greater than that of Type F steels.

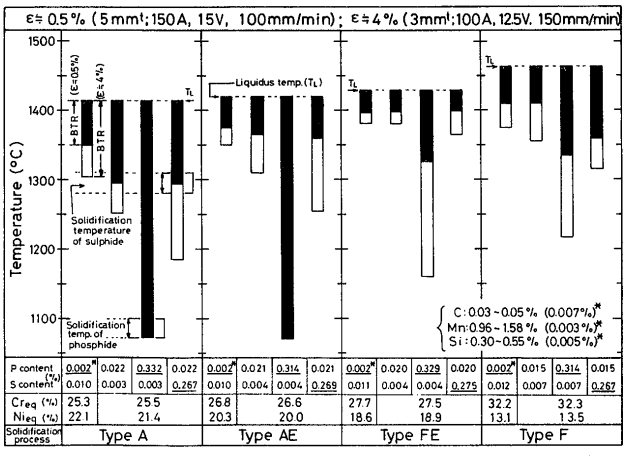

Fig. 15 Effects of P and S on BTR at ϵ=0.5 and 4% of stainless steel weld metals for each solidification process.

The effect of Type AE solidification on the segregation tendency of P and S was further examined on the TIG weld metals containing commercial P and S contents. **Figure 16** shows LM (light microscope) and SEM microstructures of Type AE (Mode IF) weld metal with about 0.021%P and 0.004%S. Phosphides identified by the EDX were observed in a granular or elliptical shape together with δ-ferrite at solidification grain and cellular dendritic boundaries in Type AE weld metal, as indicated in Fig. 16. The number of phosphides and sulphides in Type A (Mode FA) and Type AE (Mode IF) weld metals were measured as an index of the microsegregation of P and S by the SEM with the EDX. Results are tabulated in **Table 4**, together with the primary and residual δ-ferrite contents, P and S contents, the BTR values and the reference data.[11),19),22)] In the case of Type A steels shown as Heat No. A1, A2 and A3, the number of phosphides decrease remarkably with a decrease in P content, and there-

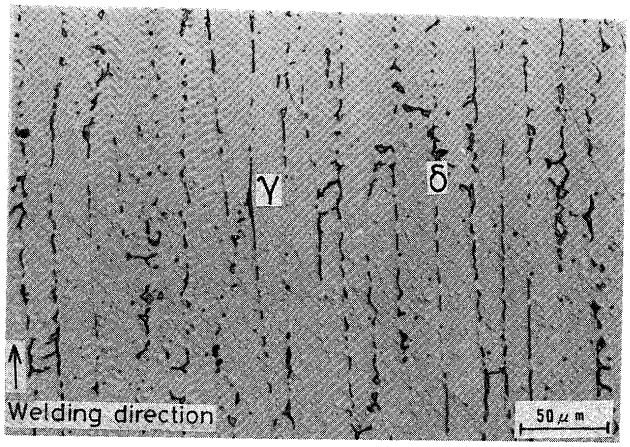

(a)

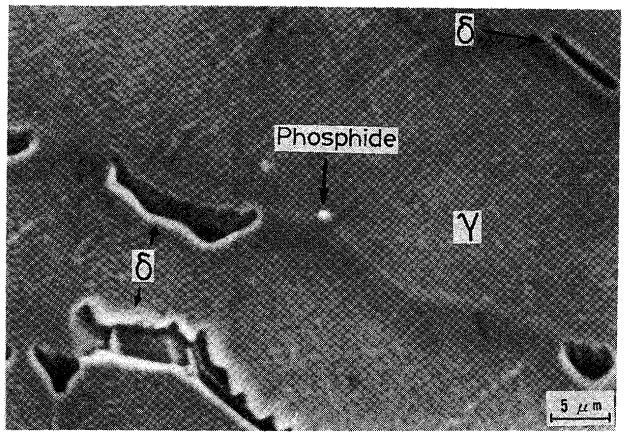

(b)

Fig. 16 Light microscope and SEM microstructures of Type AE (Mode IF) weld metal with about 0.021%P and 0.004%S, showing δ-ferrite and phosphide at boundaries.

by the cracking resistance (BTR) is improved. In the case of Type AE steels shown from Heat AE1 to Heat AE4, smaller values of the BTR are obtained in the materials with lower contents of P and S on a commercial level.

By comparison of the counts of inclusions between Type A and Type AE steels, for example, between Heat A1 and Heat AE2, it is evident that the eutectic ferrite in Type AE weld metal has a beneficial effect on the reduction in the microsegregation of P and phosphides. On careful comparison between Heat A2 or A3 and Heat AE2, the BTR of Heat AE2 steel of Type AE is narrower than that of any Type A steel in spite of higher P content and similar levels of phosphide and sulphide counts. Furthermore, the comparison of eutectic ferrite content, P and S content and the BTR between Heat AE2 and Heat AE4 or between Heat AE3 and Heat AE4 shows that the larger content of the ferrite is more beneficial to the improvement of cracking resistance, and that the beneficial effect is more remarkable for lower contents of P and S. Besides, the improved cracking resistance of Type AE steels as shown by Heat AE2 and Heat AE4 is equivalent to that of Type F (Mode WA) steels. From these results, the reason why some Type AE steels are resistant to cracking are attributed to the beneficial action of eutectic ferrite on the reduction in the microsegregation of P or the amount of low melting liquid and in addition the other essential effect. The other effect may be the resistance of δ-ferrite to cracking propagation, which will be investigated in the next section 3.4.

Table 4 Summary of primary or eutectic δ-ferrite content at solidification completion, residual δ-ferrite content at room temperature, P and S content, amount of inclusions enriched with P and/or S and BTR at ϵ=4% in weld metals with commercial levels of P and S for each solidification process.

Heat No.	Materials Compositions Creq (%)	Materials Compositions Nieq (%)	Type	Ferrite at solidification (%)	Residual ferrite (%)	Content (%) P	Content (%) S	Inclusions (count/0.096mm²) enriched in P	Inclusions (count/0.096mm²) enriched in P&S	Inclusions (count/0.096mm²) enriched in S	Inclusions (count/0.096mm²) enriched in Sum	BTR (°C)
A1	25.50	21.35	A	0	0	0.022	0.003	32	2	1	35	165
A2	25.93	22.72*	A	0	0	0.007	0.007	2	0	4	6	130
A3	25.39	21.81*	A	0	0	0.001	0.003	0	0	2	2	110
AE1	23.88	18.15	AE	2.4	1.5	0.029	0.009	14	2	2	18	155
AE2	26.57	19.97	AE	4.9	3.5	0.021	0.004	5	0	1	6	105
AE3	28.09	21.00	AE	11.9	5.9	0.025	0.009	-	-	-	-	135
AE4	29.00	21.50	AE	8.9	5.3	0.020	0.003	-	-	-	-	95
FE1	18.90	11.36*	FE	70	4.8	0.030	0.005	0	0	3	3	80
F1	30.76	15.65	F	100	30	0.017	0.006	-	-	-	-	115
F2	32.25	13.48	F	100	80	0.015	0.006	-	-	-	-	110

*According to Matsuda, et al.[19),22)] and Katayama.[11)]

3.4 Beneficial role of primary ferrite and/or eutectic ferrite on cracking resistance

From the purpose of elucidating the effect of primary and eutectic δ-ferrite on cracking resistance, the location of cracks in the microstructure and crack surfaces were observed by using cracks in the weld metals subjected to the Trans-Varestraint test. **Figure 17**(a) and (b) indicate

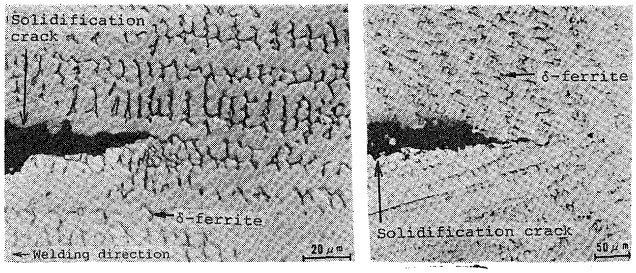

(a) (b)

Fig. 17 Light micrographs of solidification crack tips occurring at lower temperatures of BTR in Type FE weld metal (Cr_{eq}=27.5%, Ni_{eq}=18.9%, P=0.020%, S=0.004%) (a) and Type AE weld metal (Cr_{eq}=26.6%, Ni_{eq}=20.0%, P=0.021%, S=0.004%) (b), showing location of cracking path in microstructure.

solidification crack tips at lower temperature side within the BTR in Type FE and Type AE weld metals. The crack in Type FE weld metal is seen to have propagated along the migrated grain boundary forming between ferrite and austenite. Moreover, the solidification crack surfaces observed in all Type FE (Mode VF and Mode LF) materials showed the dendritic features all over the surface although the crack surfaces in Type A (Mode FA) and Type F (Mode AF, Mode WA and Mode FF) weld metals were characterized by the change from dendritic appearances to flat morphology with a temperature drop. Such observation of the location of cracks and crack surfaces are in good agreement with those reported by Matsuda, et al.[18] Therefore, the reason why the crack susceptibility of Type FE weld metals is lower than that of Type F weld metals is ascribed to the solidification process during which the migrated grain boundaries are formed between ferrite and austenite a little away from solidification grain boundaries after solidification completion and have the ductility and resistance to cracking, as the details of the mechanism were reported previously.[11),18)-22)] On the other hand, as shown in Fig. 17 (b), a crack in Type AE weld metal appears to have occurred and propagated along solidification grain boundary. δ-ferrite was frequently observed at the tips of cracks at lower temperature side in Type AE weld metals of the narrower BTR, while migrated grain boundaries were seen at crack tips in Type AE weld metals of the wider BTR.

Figure 18 (a) shows the overall solidification crack surface in Type AE weld metal with 0.029%P-0.009%S possessing the BTR of about 155°C at ϵ=4%, and Figure 18 (b) shows the crack surface at lower temperature side in Type AE weld metal with about 0.02%P-0.003% having about 95°C BTR at ϵ=4%. In the case of Type AE alloy of the wider BTR, as shown in Fig. 18 (a), crack surfaces showed apparently the dendritic features at higher temperatures and flat appearances at lower temperatures as well as those in Type A weld metals demonstrated already in other paper, but at higher magnification, a small number of traces of eutectic δ-ferrite were observed from the transient region to flat region for Type AE. On the other hand, in Type AE weld metals of narrower BTR, as seen in Fig. 18 (b), the crack surfaces indicated only dendritic features as well as those in Type FE steels. This accounts for the propagation of cracking along dendritic ferrite-austenite solidification grain boundary and migrated grain boundary. Consequently, concerning the other reason why Type AE weld metals are more resistant to cracking than Type A welds, the beneficial effect of eutectic δ-ferrite in arresting cracking propagation should be taken into consideration. Nevertheless, Type AE steels are more susceptible to cracking than Type FE materials and the

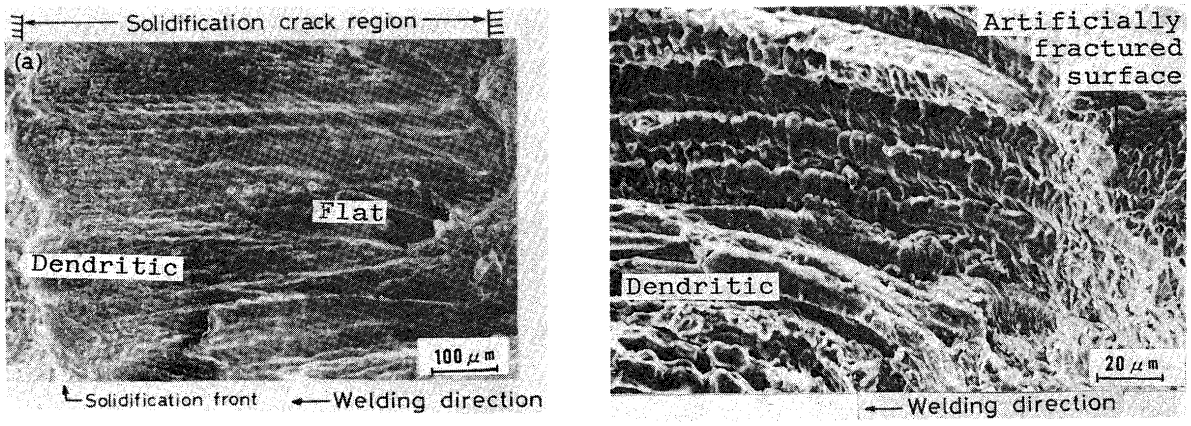

(a) (b)

Fig. 18 Solidification crack surfaces in Type AE weld metal with Cr_{eq}=23.9%, Ni_{eq}=18.2%, P=0.029%, S=0.009% (a) and with Cr_{eq}=26.6%, Ni_{eq}=20.0%, P=0.021%, S=0.004% (b).

susceptibility of Type AE steels is enhanced with commercial levels of P and S and with increases in P and S contents. As a result, the reason why Type AE steels exhibit greater susceptibility than Type FE steels may be that the degree of microsegregation of P and S is higher due to primary austenite solidification and moreover migrated grain boundaries of crack propagating paths form joining low solidification temperature liquid lakes along or near solidification grain boundaries.

The above-mentioned results confirm that the cracking susceptibility of stainless steels can be interpreted by considering the behavior of migrated grain boundaries and their correlation to δ-ferrite and liquids enriched with P and S at the super- and sub-solidus temperatures as well as the effect of the primary solidification of ferrite or austenite in reducing the microsegregation of P and S during solidification.

4. Conclusions

This study was performed on a wide variety of stainless steels not only to elucidate the effect of primary and eutectic δ-ferrite on cracking resistance but also to obtain fundamentals of the development of a crack-resistant stainless steel by defining a correlation between solidification process, microstructure, microsegregation and cracking susceptibility. The following conclusions were drawn by cracking tests and metallographic investigation:

(1) On the basis of the interpretation of Fe-Cr-Ni ternary diagram and observation results of microstructures of weld metals quenched rapidly from high temperatures during TIG welding and normal weld metals cooled continuously to room temperature after welding, stainless steel weld metals were classified into five different types of solidification processes and correspondingly eight characteristic microstructural modes: Type A (austenitic single-phase solidification) –Mode FA (fully austenitic (cellular dendritic) microstructure); Type AE (primary austenite and eutectic austenite-ferrite solidification) – Mode IF (intercellular eutectic ferrite at solidification grain boundaries); Type E (eutectic austenite-ferrite solidification) – Mode EF (dendritic or island-like eutectic ferrite); Type FE (primary ferrite and eutectic ferrite-austenite solidification) – Mode VF (vermicular, skeletal or dendritic ferrite in primary cellular dendrite cores) or Mode LF (lacy ferrite in primary cellular dendrite axes); Type F (ferritic single-phase solidification) – Mode AF (acicular ferrite within columnar grain surrounded with austenite along grain boundaries), Mode WA (feathery Widmanstätten austenite growing from grain boundary austenite with no transformation ferrite region in the center of grain) or Mode FF (fully ferritic microstructure without any precipitation of austenite).

(2) The compositional regions of distinct solidification processes and related characteristic microstructural modes could be illustrated in the Schaeffler diagram.

(3) It was noted that the formation mechanism of a small content of residual δ-ferrite at room temperature for lower $Cr_{eq}+Ni_{eq}$ was different from that for higher $Cr_{eq}+Ni_{eq}$. For example, about 5% δ-ferrite was retained in the shape of Mode VF and/or Mode LF from primary δ-ferrite in cell axes for lower $Cr_{eq}+Ni_{eq}$, while it resulted from eutectic ferrite at solidification grain and cellular dendritic boundaries as Mode IF for higher $Cr_{eq}+Ni_{eq}$.

(4) According to the BTR obtained by the Trans-Varestraint test, solidification cracking susceptibility of stainless steels with commercial levels of P and S depended largely upon the compositions of weld metals; or more exactly, it was dependent on the solidification process. That is to say, Type A steels exhibited the highest susceptibility to weld cracking, Type F materials were more resistant, and Type FE steels possessed the greatest resistance to cracking. For Type AE solidification, some steels were susceptible to cracking but the others were as resistant as or more resistant than Type F materials.

(5) It was recognized that there existed a close correlation between the BTR (cracking susceptibility) and residual δ-ferrite content when the relations were treated separately for lower and higher $Cr_{eq}+Ni_{eq}$, since residual δ-ferrite content was connected with solidification processes.

(6) It was revealed that an austenitic stainless steel with commercial levels of P and S contents containing only 2% residual δ-ferrite on lower Cr_{eq} side for lower $Cr_{eq}+Ni_{eq}$ was fairly resistant to cracking due to Type FE solidification.

(7) Backfilled (healed) cracks were frequently observed at an augmented-strain of 0.5% and complete healing of cracks was recognized especially in short cracks in Type FE weld metals having very narrow BTR.

(8) Cracks were absent in TIG arc spot nuggets of Type FE, Type F and some Type AE solidification processes showing the BTR of 55°C or less ϵ=0.5%, and 110°C or less at ϵ=4%, and no cracks were observed in cross sections of resistance spot weld metals of Type FE solidification showing the BTR of less than 40 and 80°C at ϵ=0.5 and 4%, respectively. It was thus confirmed that cracking propensities in practical cases were closely associated with the solidification process in agreement with the BTR evaluation.

(9) According to the investigation results of microsegregation of P and S in weld metals with about 0.33%P or 0.27%S, phosphides enriched with P, Fe, Cr, Ni, etc. were observed in a film-like form along solidification grain boundaries and in a rod-like shape at cellular dendritic boundaries for Type A and Type AE solidification, while sulphides enriched with S, Mn and Cr were found in a globular or rod-like form at solidification grain and cellular dendritic boundaries for any solidification process.

(10) From the measured results of phosphide and sulphide contents it was confirmed that primary δ-ferrite in Type FE and Type F solidification have a great beneficial effect in decreasing the microsegregation of P in particular and S, and that eutectic δ-ferrite in Type AE also have a slight but obvious effect on the reduction in P microsegregation or phosphide formation.

(11) Based on the cracking test results of stainless steels with P and S addition and Fe-Cr-Ni ternary alloys with very low P content, S addition increased the cracking susceptibility of weld metals to some extent for any solidification process whilst P addition was extremely detrimental for primary austenite solidification of Type A and Type AE. Moreover, it was confirmed that the decrease in P content was very effective in reducing cracking susceptibility especially for Type A and Type AE materials.

(12) Type F (Mode WA) materials showed a greater resistance to cracking than Type A (Mode FA) steels for commercial and intentionally added levels of P and S content. The reason was readily understood in terms of the beneficial effect of primary δ-ferrite solidification in reducing microsegregation of P in particular and S.

(13) In Type FE (Mode VF or Mode LF) weld metals, solidification crack surfaces showed only dendritic feature all over the face, crack tips at lower temperatures of the BTR at large strains were observed along the boundaries between austenite and ferrite, and completely backfilled cracks were found in short cracks. On the basis of the metallographic observation results, the reason why the best cracking resistance could be achieved in some Type FE weld metals was attributed to three primary effects: One was that primary δ-ferrite had a beneficial effect in reducing the segregation of P in particular and S, another was that irregular (migrated) grain boundaries formed during solidification and subsequent cooling had enough ductility to arrest the propagation of cracking, and the other was that healing cracks prevailed due to short crack length or narrow BTR.

(14) In some Type AE weld metals, crack surfaces were generally characterized by dendritic appearance and δ-ferrite of Mode IF was observed at crack tips. Consequently the reason why Type AE weld metals were more resistant to cracking to Type A ones was revealed to be ascribed to the beneficial effects of eutectic δ-ferrite in arresting cracking propagation and in reducing the microsegregation of P in particular to a considerable degree. However, Type AE welds were more susceptible than Type FE, probably because the degree of impurity segregation was higher due to the primary austenite solidification and moreover migrated grain boundaries of crack propagating paths were formed joining low melting liquid lakes along or in solidification grain boundaries.

Acknowledgements

The authors wish to thank Prof. Dr. F. Matsuda of JWRI, Osaka University for his valuable discussion and the use of the Trans-Varestraint test, since this study was based on the fundamental knowledge obtained under the direction of Prof. F. Matsuda. The authors also would like to acknowledge Mr. A. Yamaguchi and Mr. K. Kishimoto of Sanyo Special Steel Company, Ltd. for their supplying materials and analyzing alloys.

References

1) J.C. Borland and R.N. Younger: Brit. Weld. J., Vol. 7 (1960), No. 1, 22–59.

2) J. Honeycombe and T.G. Gooch: Metal Constr. and Brit. Weld. J., Vol. 5 (1973), No. 4, 140–147.

3) F.C. Hull: Welding J., Vol. 46 (1967), No. 9, 399s–409s.

4) Y. Arate, F. Matsuda and S. Saruwatari: Trans. of JWRI, Vol. 3 (1974), No. 1, 79–88.

5) S. Kawashima, Y. Aoyama, F. Fukui, S. Inoue and K. Harada: Tetsu-to-Hagane (Journal of ISIJ), Vol. 62 (1976), No. 10, 1386–1391 (in Japanese).

6) C.D. Lundin, W.T. DeLong and D.F. Spond: Welding J., Vol. 54 (1975), No. 8, 241s–246s.

7) C.D. Lundin, W.T. DeLong and D.F. Spond: Welding J., Vol. 55 (1976), No. 6, 145s–151s.

8) J.A. Brooks and F.J. Lambert: Welding J., Vol. 57 (1978), No. 5, 139s–143s.

9) J. Honeycombe and T.G. Gooch: Metal Constr. and Brit. Weld. J., Vol. 2 (1970), No. 9, 375–380.

10) Y. Arata, F. Matsuda, H. Nakagawa, S. Katayama and S. Ogata: Trans. of JWRI, Vol. 6 (1977), No. 2, 197–206.

11) S. Katayama: Ph. D. Thesis, Osaka University, Oct. 1981 (in Japanese).

12) C.D. Lundin and D.F. Spond: Welding J., Vol. 55 (1976), No. 11, 356s–367s.

13) J. Honeycombe and T.G. Gooch: Metal Constr. and Brit. Weld. J., Vol. 4 (1972), No. 12, 456–460.

14) I. Masumoto, K. Tamaki and M. Kutsuna: J. of JWS, Vol. 41 (1972), No. 11, 1306–1314 (in Japanese).

15) Y. Arata, F. Matsuda and S. Katayama: Trans. of JWRI, Vol. 5 (1976), No. 2, 135–151.

16) Y. Arata, F. Matsuda and S. Katayama: Trans. of JWRI, Vol. 6 (1977), No. 1, 105–116.

17) Y. Arate, F. Matsuda, H. Nakagawa and S. Katayama: Trans. of JWRI, Vol. 7 (1978), No. 2, 169–172.

18) F. Matsuda, H. Nakagawa, T. Uehara, S. Katayama and Y. Arata: Trans. of JWRI, Vol. 8 (1979), No. 1, 105–112.

19) F. Matsuda, S. Katayama and Y. Arata: Trans. of JWRI, Vol. 10 (1981), No. 2, 201–212.

20) F. Matsuda, H. Nakagawa, S. Katayama and Y. Arata: Trans. of JWS, Vol. 13 (1982), No. 2, 115–132.

21) F. Matsuda, H. Nakagawa and S. Katayama: IIW-Doc. IX-1315-84, 1–21.

22) F. Matsuda, H. Nakagawa, S. Katayama and Y. Arata: Trans. of JWRI, Vol. 12 (1983), No. 1, 89–95.

23) F. Matsuda, H. Nakagawa, S. Ogata and S. Katayama: Trans. of JWRI, Vol. 7 (1978), No. 1, 59–70.

24) F. Matsuda, H. Nakagawa, S. Katayama and Y. Arata: Trans. of JWRI, Vol. 11 (1982), No. 1, 79–94.

25) F. Matsuda, H. Nakagawa, S. Katayama and Y. Arata: Trans. of JWRI, Vol. 11 (1982), No. 2, 79–85.

26) F. Matsuda, S. Katayama and Y. Arata: Trans. of JWRI, Vol. 12 (1983), No. 2, 247–252.

27) T. Takalo, N. Suutala and T. Moisio: Metallurgical Trans., Vol. 10A (1979), No. 8, 1173–1181.

28) N. Suutala, T. Takalo and T. Moisio: Metallurgical Trans., Vol. 10A (1979), No. 8, 1183–1190.

29) N. Suutala, T. Takalo and T. Moisio: Metallurgical Trans.: Vol. 11A (1980), No. 5, 717–725.

30) V. Kujanpää, N. Suutala, T. Takalo and T. Moisio: Welding Research International, Vol. 9 (1979), No. 2, 55–76.

31) V.P. Kujanpää, N.J. Suutala, T.K. Takalo and T.J.I. Moisio: Metal Construction, (1980), No. 6, 282–285.

32) V.P. Kujanpää: Metal Construction, (1985), No. 1, 40R–46R.

33) J.C. Lippold and W.F. Savage: Welding J., Vol. 58 (1979), No. 12, 362s–374s.

34) J.C. Lippold and W.F. Savage: Welding J., Vol. 59 (1980), No. 2, 48s–58s.

35) J.C. Lippold and W.F. Savage: Welding J., Vol. 61 (1982), No. 12, 388s–396s.

36) J.A. Brooks, J.C. Williams and A.W. Thompson: Metallurgical Trans., Vol. 14A (1983), No. 1, 23–31.

37) J.A. Brooks, J.C. Williams and A.W. Thompson: Metallurgical Trans., Vol. 14A (1983), No. 7, 1271–1281.

38) J.A. Brooks, A.W. Thompson and J.C. Williams: Welding. J., Vol. 63 (1984), Vol. 4, 71s–83s.

39) S.A. David, G.M. Goodwin and D.N. Braski: Welding J., Vol. 58 (1979), No. 12, 330s–336s.

40) S.A. David: Welding J., Vol. 60 (1981), No. 4, 63s–71s.

41) G.L. Leone and H.W. Kerr: Welding J., Vol. 61 (1982), No. 4, 13s–21s.

42) A.L. Schaeffler: Metal Progress, Vol. 56 (1949), No. 5, 680–680B.

43) T. Senda, F. Matsuda, G. Takano, K. Watanabe, T. Kobayashi and T. Matsuzaka: Trans. of JWS, Vol. 2 (1971), No. 2, 1–12.

44) C.H.M. Jenkins, E.H. Bucknall, C.R. Austin and G.A. Meller: J. Iron & Steel Inst., Vol. 136 (1937), 187–222.

45) E. Schümann and J. Brauckmann: Arch. Eisenhüttenwes., Vol. 48 (1977), No. 1, 3–7.

46) V.G. Rivlin and G.V. Raynor: International Metals Reviews, (1980), No. 1, 21–38.

47) T. Okamoto, K. Kishitake and K. Murakami: Trans. ISIJ, Vol. 21 (1981), 641–648.

48) S. Katayama: unpublished research performed at JWRI of Osaka University.

49) J.W. Pugh and J.D. Nisbet: Trans. of AIME, Vol. 188 (1950), No. 2, 268–276.

50) M.J. Cieslak and W.F. Savage: Welding J., Vol. 59 (1980), No. 5, 136s–146s.

51) M.J. Cieslak, A.M. Ritter and W.F. Savage: Welding J., Vol. 61 (1982), No. 1, 1s–8s.

52) J.M. Vitek, A. Dasgupta and S.A. David: Metallurgical Trans., Vol. 14A (1983), No. 9, 1833–1841.

53) W.T. DeLong: Welding J., Vol. 53 (1974), No. 7, 273s–286s.

54) T.F. Kelly, M. Cohen and J.B.V. Sande: Metallurgical Trans., Vol. 15A (1984), No. 5, 819–833.

55) S. Katayama and A. Matsunawa: Proc. of ICALEO, Vol. 44 (1984), 60 – 67.

56) N. Suutala, T. Takalo and T. Moisio: Welding J., Vol. 60 (1981), No. 5, 92s–93s.

57) W.I. Pumphrey and P.H. Jennings: J. Inst. Met., Vol. 75 (1948), 235–256.

58) J.C. Borland: Brit. Weld. J., Vol. 7 (1960), 508–512.

59) H. Nakagawa, F. Matsuda and T. Senda: Trans. of JWS, Vol. 5 (1974), No. 1, 39–46.